Eur. Phys. J. C 27, 555–561 (2003)
Digital Object Identifier (DOI) 10.1140/epjc/s2003-01154-0

THE EUROPEAN PHYSICAL JOURNAL C

Effect of fourth generation CP phase on $b \to s$ transitions

A. Arhrib[1,2], W.-S. Hou[3]

[1] Max-Planck Institut für Physik, Föhringer Ring 6, 80805 München, Germany
[2] LPHEA, Physics Department, Faculty of Science-Semlalia, P.O.B. 2390, Marrakesh, Morocco
[3] Department of Physics, National Taiwan University, Taipei, Taiwan 10764, R.O.C.

Received: 20 November 2002 /
Published online: 7 March 2003 –

Abstract. We study the effect of a sequential fourth generation on $b \to s\gamma$, B_s mixing, $B \to K^{(*)}\ell^+\ell^-$, $X_s\ell^+\ell^-$ and $\phi K_{\rm S}$, taking into account the presence of a new CP phase in quark mixing. We find that the effects via electromagnetic and strong penguins, such as in $b \to s\gamma$ or CP-violation in $B \to \phi K_{\rm S}$, are rather mild, but the impact via boxes or Z penguins is quite significant. Not only can one have a B_s mixing much larger than expected, even if it is measured near the present limit, mixing-dependent CP-violation could become maximal. For electroweak penguin modes, the fourth generation can provide the enhancement that perhaps may be needed, while the $m_{\ell^+\ell^-}$ dependence of the forward–backward asymmetry in $B \to K^*\ell^+\ell^-$ can further probe for the fourth generation. These effects can be studied in detail at the B factories and the Tevatron.

1 Introduction

The source of CP-violation within the standard model lies in the Cabibbo–Kobayashi–Maskawa (CKM) quark mixing matrix, where a unique KM phase emerges with three generations of quarks and leptons. Despite its great success, there are reasons to believe that the three generation standard model (SM, or SM3) may be incomplete. For example, the generation structure is not understood, while recent observations of neutrino oscillations point towards an enlarged neutrino sector [1]. A simple enlargement is to add a sequential fourth generation (SM4); with additional mixing elements, one crucial aspect is that the source for CP-violation is no longer unique.

The B factories at KEK and SLAC have turned on with a splash, and CP-violation has been observed in $B^0 \to J/\psi K_{\rm S}$ decay modes which is consistent with SM3. Both experiments have recently observed the $B \to K\ell^+\ell^-$ [2–5] decay mode, while the Belle Collaboration has just reported the observation of the inclusive $B \to X_s\ell^+\ell^-$ mode [6]. Though a bit on the high side, the results are again not inconsistent with SM3. However, there may be a hint for new physics in the mixing-dependent CP-violation in $B^0 \to \phi K_{\rm S}$ decay [7]. At any rate, together with many related loop-induced processes, we have entered an age where the uniqueness of the three generation SM phase can start to be checked.

The $B \to K\ell^+\ell^-$ type of decays are highly suppressed in the SM because they occur only via electroweak penguin processes. The first measurement of such processes through $b \to s\gamma$ was performed some years ago by CLEO [8]. The measured branching ratio has been used to constrain the Wilson coefficient $|C_7^{\rm eff}|$ [9]. The measurement of the $B \to (K,\ K^*)\ell^+\ell^-$ and $X_s\ell^+\ell^-$ modes can provide information on $C_9^{\rm eff}$ and C_{10}, as well as sign information on $C_7^{\rm eff}$.

The contributions from the fourth generation to rare decays have been extensively studied [10–13], where the measured $b \to s\gamma$ decay rate has been used [13] to put stringent constraints on the additional CKM matrix elements. However, most of these studies neglect the effect of new CP phases by taking $\lambda_{t'} \equiv V_{t's}^* V_{t'b}$ to be real. The $b \to s\gamma$ constraint then implies that, for fixed t' quark mass, $\lambda_{t'}$ can take on only one of two values.

In this paper, we study the effect of the fourth generation on $b \to s$ transitions by including the CP phase in $V_{t's}^* V_{t'b}$. We use the updated measured value of $b \to s\gamma$ [15] and the lower bound on B_s^0–$\bar{B}_s^0$ mixing, to put a constraint on fourth generation parameters. The effect of the allowed region of parameter space on $b \to s$ transitions are compared with Belle and BaBar measurements. We further discuss the forward–backward asymmetry of $B \to (K,\ K^*)\ell^+\ell^-$, and indirect CP-violation in B_s–$\bar{B}_s$ mixings and $B^0 \to \phi K_{\rm S}$ decay. We stress that we focus on $V_{t's}^* V_{t'b}$ only, in anticipation of new data. Thus, only one additional new CP phase is introduced. The $K^+ \to \pi^+\nu\bar{\nu}$ process, B_d mixing and its CP phase etc., involve $V_{t'd}^* V_{t's}$, $V_{t'd}^* V_{t'b}$ respectively, which are quite independent from the CP phase information contained in $V_{t's} V_{t'b}$.

2 Strategy

The $b \to s\gamma$ process provides a stringent constraint on new physics, while the non-observation of B_s–$\bar{B}_s$ mixing also puts constraints on a fourth generation. We shall discuss these two traditional constraints before turning to more recent experimental observations.

2.1 The $b \to s\gamma$ constraint

With a sequential fourth generation, the Wilson coefficients C_7 and C_8 receive contributions from the t' quark loop, which we will denote as $C_{7,8}^{\rm new}$. Because a sequential fourth generation couples in a similar way to the photon and W, the effective Hamiltonian relevant for $b \to s\gamma$ decay has the following form:

$$\mathcal{H}_{\rm eff} = \frac{4G_{\rm F}}{\sqrt{2}} \sum_{i=1}^{i=8} [\lambda_t C_i^{\rm SM}(\mu) + \lambda_{t'} C_i^{\rm new}(\mu)] O_i(\mu), \quad (1)$$

with $\lambda_f = V_{fs}^* V_{fb}$, and the O_is are just as in SM. The unitarity of the 4×4 CKM matrix leads to $\lambda_u + \lambda_c + \lambda_t + \lambda_{t'} = 0$. Taking into account that λ_u is very small compared to the others, one has [10,11]

$$\lambda_t \cong -\lambda_c - \lambda_{t'}, \quad (2)$$

and $\lambda_c = V_{cs}^* V_{cb}$ is real by convention. It follows that

$$\lambda_t C_{7,8}^{\rm SM} + \lambda_{t'} C_{7,8}^{\rm new} = -\lambda_c C_{7,8}^{\rm SM} + \lambda_{t'} (C_{7,8}^{\rm new} - C_{7,8}^{\rm SM}), \quad (3)$$

where the first term corresponds to the usual SM contribution. It is clear that, for the $m_{t'} \to m_t$ and $\lambda_{t'} \to 0$ limits, the $\lambda_{t'}(C_{7,8}^{\rm new} - C_{7,8}^{\rm SM})$ term vanishes, as required by the GIM mechanism. We parameterize

$$\lambda_{t'} \equiv r_s \, {\rm e}^{{\rm i}\Phi_s}, \quad (4)$$

where Φ_s is a new CP-violating phase.

The branching ratio of $b \to s\gamma$ is computed by using formulas given in [16]. Using $\mathcal{B}(B \to X_c e \bar{\nu}_e) = 10.4\%$, $\lambda_c = 0.04$, we find $\mathcal{B}(B \to X_s\gamma) \simeq 3.26 \times 10^{-4}$ in SM. The present world average for $B \to X_s\gamma$ rate is [15],

$$\mathcal{B}(B \to X_s\gamma) = (3.3 \pm 0.4) \times 10^{-4}. \quad (5)$$

We will keep the $b \to s\gamma$ branching ratio in the 1σ range of $(2.9\text{–}3.7) \times 10^{-4}$ in the presence of a fourth generation.

We note that the CDF Collaboration excludes [17] the b' quark in the mass range of $100\,{\rm GeV} < m_{b'} < 199\,{\rm GeV}$ at 95% C.L., if $\mathcal{B}(b' \to bZ) = 100\%$[1]. Precise EW data provide a stringent constraint on the fourth generation: the splitting between t' and b' is severely constrained by $|m_{t'} - m_{b'}| \le m_Z$ [15,18,19]. Assuming that $m_{t'} > m_{b'}$, we conclude that the t' should be heavier than $\approx 199\,{\rm GeV} + m_Z$. In our analysis we will consider only a t' heavier than 250 GeV.

In Fig. 1 we give a contour plot of $\mathcal{B}(B \to X_s\gamma)$ in the (Φ_s, r_s) plane for $m_{t'} = 250$ and 350 GeV. We see that the CP phase Φ_s does make a considerable impact on the range of $\mathcal{B}(B \to X_s\gamma)$, but one not particularly sensitive to $m_{t'}$. In general, for both the $m_{t'} = 250$ and 350 GeV cases, r_s cannot be much larger than 0.02 if one wishes to keep $\mathcal{B}(B \to X_s\gamma)$ in the range of $(2.9\text{–}3.7) \times 10^{-4}$. But for $\Phi_s \sim \pi/2, 3\pi/2$, *when* $V_{t's}^* V_{t'b}$ *is largely imaginary*, r_s can take on much larger values; for these cases the t' contribution

[1] Such a limit can be relaxed [18] if we consider that the decays $b' \to bH$ and $b' \to cW$ may be competitive with $b' \to bZ$

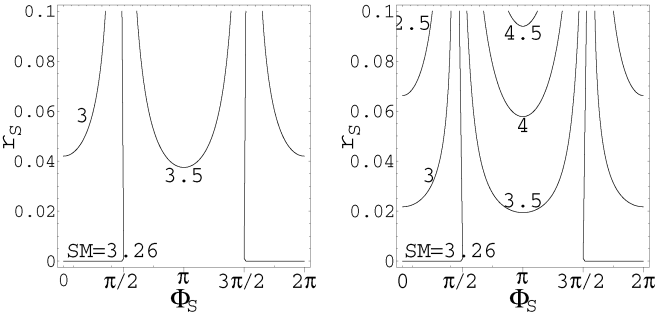

Fig. 1. Contours for $\mathcal{B}(B \to X_s\gamma)(\times 10^4)$ in the (Φ_s, r_s) plane, for $m_{t'} = 250$ (350) GeV on the left (*right*)

adds only in quadrature to the SM contribution, hence is much more accommodating. In this sense, our approach is different from the approach of [10,13] where $\lambda_{t'}$ is taken as real, and can take on only one of two values for a fixed $m_{t'}$.

Since the chiral structure is the same as in SM, and since a heavy state such as t' does not bring in extra absorptive parts, CP asymmetry in $b \to s\gamma$ remains small.

However, the possibility of sizable CP odd t' contributions allowed by $b \to s\gamma$, while not easily distinguished in the $b \to s\gamma$ process itself, can make an impact on CP observables in other $b \to s$ transitions, as we shall see.

2.2 B_s^0–$\bar{B}_s^0$ mixing constraint

Because of a strong $m_{t'}$ dependence, the fourth generation contribution can easily have an impact on B_s^0–$\bar{B}_s^0$ mixing and its CP phase Φ_{B_s}, and can be accessible soon at the Tevatron Run II.

We use the definition of $\Delta m_{B_s} = 2|M_{12}^B|$ and $M_{12}^B = |M_{12}^B| {\rm e}^{{\rm i}\Phi_{B_S}}$, where M_{12}^B is given by [20]

$$M_{12}^B = \frac{G_{\rm F}^2 M_W^2}{12\pi^2} M_{B_s} B_{B_s} f_{B_s}^2 \{\lambda_t^2 \eta S_0(x_{tW}^2) + \eta' \lambda_{t'}^2 S_0(x_{t'W}^2) + 2\widetilde{\eta}' \, \lambda_t \, \lambda_{t'} \, \widetilde{S}_0(x_{tW}^2, x_{t'W}^2)\}, \quad (6)$$

with $x_{fW} = m_f/M_W$, and

$$S_0(x) = \frac{4x - 11x^2 + x^3}{4(1-x)^2} - \frac{3}{2}\frac{\log x x^3}{(1-x)^3}, \quad (7)$$

$$\frac{\widetilde{S}_0(x,y)}{xy} = \left\{ \frac{1}{y-x}\left[\frac{1}{4} + \frac{3}{2}\frac{1}{1-y} - \frac{3}{4}\frac{1}{(1-y)^2}\right]\log y + \frac{1}{x-y}\left[\frac{1}{4} + \frac{3}{2}\frac{1}{(1-x)} - \frac{3}{4}\frac{1}{(1-x)^2}\right]\log x - \frac{3}{4}\frac{1}{(1-x)(1-y)} \right\}, \quad (8)$$

where $\eta = 0.55$ is the QCD correction factor. Taking into account the threshold effect from the b' quark, we find

$$\eta' = \alpha_{\rm s}(m_t)^{6/23} \left(\frac{\alpha_{\rm s}(m_{b'})}{\alpha_{\rm s}(m_t)}\right)^{6/21} \left(\frac{\alpha_{\rm s}(m_{t'})}{\alpha_{\rm s}(m_{b'})}\right)^{6/19}.$$

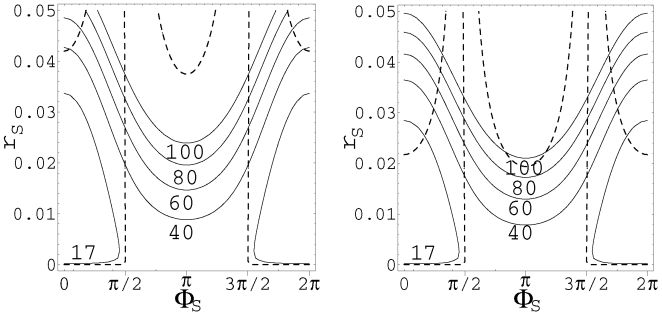

Fig. 2. Contours for Δm_{B_s} (ps^{-1}) in the (Φ_s, r_s) plane, for $m_{t'} = 250(350)\,\mathrm{GeV}$ on the left (*right*), with the results of Fig. 1 overlayed as dashed lines for comparison

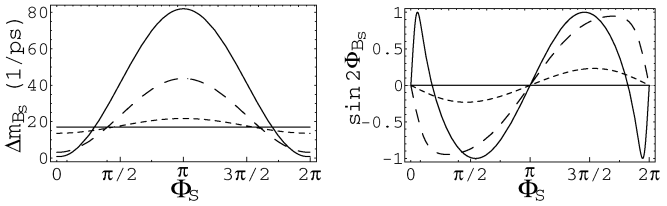

Fig. 3. Δm_{B_s} (*left*) and $\sin 2\Phi_{B_s}$ (*right*) versus Φ_s for $m_{t'} = 250\,\mathrm{GeV}$ and $r_s = 0.002$ (short dash), 0.01 (long dash) and 0.02 (solid)

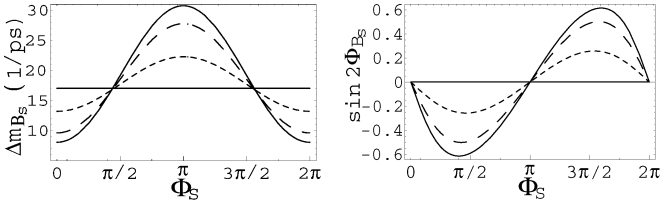

Fig. 4. Same as Fig. 3 for $m_{t'} = 350\,\mathrm{GeV}$ and $r_s = 0.002$ (*short dash*), 0.004 (*long dash*) and 0.005 (*solid*)

Given the splitting between t' and b', it turns out that η' is also close to 0.55 for $250\,\mathrm{GeV} < m_{t'} < 350\,\mathrm{GeV}$, which is not surprising. We shall take $\widetilde{\eta}' = \eta'$.

In our calculation we use $B_{B_s} f_{B_s}^2 = (260\,\mathrm{MeV})^2$ and $\overline{m}_t(m_t) = 168\,\mathrm{GeV}$, which gives $\Delta m_{B_s}^{\mathrm{SM}} \simeq 17.0\,\mathrm{ps}^{-1}$ with vanishing $\sin 2\Phi_{B_s}^{\mathrm{SM}}$. For illustration, in Fig. 2 we give a contour plot of Δm_{B_s} in the (Φ_s, r_s) plane, for $m_{t'} = 250$ and 350 GeV. The result of Fig. 1 is overlayed for comparison. We see that Δm_{B_s} can reach $90\,\mathrm{ps}^{-1}$ for $r_s \approx 0.02$ and $\Phi_s \approx \pi$, but for heavier $m_{t'}$, $\mathcal{B}(B \to X_s\gamma)$ will reach beyond 3.7×10^{-4} and become less likely. For $\Phi_s \sim \pi/2$, $3\pi/2$, where $b \to s\gamma$ is more tolerant, Δm_{B_s} can get greatly enhanced. On the other hand, the experimental lower bound of $\Delta m_{B_s} > 14.9\,\mathrm{ps}^{-1}$ implies that the region where $0 \le r_s \le 0.03$ and $\cos\Phi_s > 0$ is disfavored, which rules out a region allowed by $b \to s\gamma$. We now see that the allowed parameter space is larger for the $m_{t'} = 250\,\mathrm{GeV}$ case, i.e. for heavier $m_{t'}$, r_s can only take on smaller values. This is because the $m_{t'}$ dependence for Δm_{B_s} is rather strong, but is much weaker in case of $b \to s\gamma$.

We stress that the $\Phi_s \sim \pi/2, 3\pi/2$ cases are much more forgiving because the CP phase for $b \to s$ transitions is practically real in SM3, hence a purely imaginary fourth generation contribution adds only in quadrature. We thus turn to the study of the possible impact of a fourth generation, especially through its new CP phase, on other $b \to s$ transitions.

3 CP-violation in B meson mixing

Here we mean B_s^0–$\bar{B}_s^0$ mixing. A fourth generation can affect B_d^0–$\bar{B}_d^0$ mixing and its CP phase through $V_{t'd}^* V_{t'b}$. Since there is no apparent deviation from SM3 [15] expectations, we ignore it.

While an enhanced Δm_{B_s} can easily evade present bounds, of particular interest is whether and how a fourth generation could affect the mixing-dependent CP-violating observable $\sin 2\Phi_{B_s}$, which is analogous to the recently measured CP phase in the B_d^0–$\bar{B}_d^0$ mixing amplitude. We plot Δm_{B_s} and $\sin 2\Phi_{B_s}$ versus Φ_s in Figs. 3 and 4, for $m_{t'} = 250$ and 350 GeV, respectively, for several values of r_s. In general, the interference between SM3 and fourth generation effects is constructive for $\cos\Phi_s < 0$, and can enhance Δm_{B_s} up to 80–$90\,\mathrm{ps}^{-1}$ for large $r_s \approx 0.02$, as we have seen already in Fig. 2. Conversely, destructive interference occurs for $\cos\Phi_s > 0$, but this would give $\Delta m_{B_s} < \Delta m_{B_s}^{\mathrm{SM}}$, hence is disfavored by the present lower bound. We are thus more interested in the constructive interference scenario, or when $\Phi_s \sim \pi/2$, $3\pi/2$, where the $b \to s\gamma$ and Δm_{B_s} constraints are more forgiving.

We illustrate the $m_{t'} = 250\,\mathrm{GeV}$ case with a larger range of r_s values. This not only allows for a greatly enhanced Δm_{B_s}, it makes $\sin 2\Phi_{B_s}$ very interesting. We see from Fig. 3 that the $\sin 2\Phi_{B_s}$ structure is rich: for $r_s > 0.01$, $\sin 2\Phi_{B_s}$ can reach $\pm 100\%$. This can be traced to the dependence of M_{12} on Φ_s. We see from (6) that the $\lambda_{t'}^2$, $\lambda_{t'}$, and $\lambda_{t'}$-independent terms imply that M_{12} takes the following form:

$$M_{12} = |M_{12}| \mathrm{e}^{2\mathrm{i}\Phi_{B_s}} \approx r_s^2 \mathrm{e}^{2\mathrm{i}\Phi_s} A + r_s \mathrm{e}^{\mathrm{i}\Phi_s} B + C, \qquad (9)$$

where A and B are explicit functions of m_t and $m_{t'}$ and C is the usual SM3 contribution. For large enough r_s, the $r_s^2 \mathrm{e}^{2\mathrm{i}\Phi_s}$ term dominates, and one has $\mathrm{e}^{2\mathrm{i}\Phi_s}$ modulation. But as r_s decreases, the quadratic term becomes unimportant, and our term is only subject to the $\mathrm{e}^{\mathrm{i}\Phi_s}$ modulation arising from the interference term.

Thus, *for r_s as small as 0.002* (compare $|\lambda_c| = |V_{cs}^* V_{cb}| \cong 0.04$), *$\Delta m_{B_s}$ is close to the SM3 value, but* $\sin 2\Phi_{B_s}$ *can already reach* $\mp 25\%$ near $\Phi_s = \pi/2$, $3\pi/2$. For $r_s = 0.01$, Φ_s is restricted by the Δm_{B_s} lower bound to the range of $70^\circ \lesssim \Phi_s \lesssim 300^\circ$, where $\sin 2\Phi_{B_s}$ can take on *extremal values* of $\mp 100\%$ near the boundaries. This is very interesting, for *if Δm_{B_s} is measured soon near the present bounds, we may find the associated CP-violating phase to be maximal!* For $r_s = 0.02$, the allowed range for Φ_s is slightly larger than (roughly $50^\circ \lesssim \Phi_s \lesssim 310^\circ$) the $r_s = 0.01$ case. The maximal $\sin 2\Phi_{B_s}$ now occurs close to $\Phi_s = \pi/2$, $3\pi/2$ since the fourth generation effect overwhelms the SM3 top quark effect. In all these cases, $\sin 2\Phi_{B_s}$ vanishes for $\Phi_s = \pi$ when one has maximal constructive interference in Δm_{B_s}.

It should be noted that, for purely imaginary $e^{i\Phi_s}$, r_s could be considerably larger than 0.02, leading to a very large Δm_{B_s} and maximal $\sin 2\Phi_{B_s}$. The measurements of such cases, however, are more difficult.

For the heavier $m_{t'} = 350\,\text{GeV}$ scenario of Fig. 4, $b \to s\gamma$ puts a slightly tighter constraint, hence we have illustrated the Φ_s dependence of Δm_{B_s} and $\sin 2\Phi_{B_s}$ for r_s only up to 0.005. For this parameter space, the $r_s^2 e^{2i\Phi_s}$ term in (9) is subdominant, and one largely has $e^{i\Phi_s}$ modulation. The case is similar to the low r_s discussion of Fig. 3. Once again, for $\Phi_s \sim \pi/2$, $3\pi/2$, r_s could be much larger than the illustrated range, and $\sin 2\Phi_{B_s}$ would become maximal.

4 Electroweak penguin $B \to (K, K^*)\ell^+\ell^-$

A recent highlight from B factories is the emerging electroweak penguins. Based on $30\,\text{fb}^{-1}$ data, the first observation of $B \to K\mu^+\mu^-$ was reported by the Belle experiment in 2001, giving $\mathcal{B}(B \to K\mu^+\mu^-) = (0.99^{+0.40+0.13}_{-0.32-0.14}) \times 10^{-6}$ [2]. This was updated [3] in 2002 to $(0.80^{+0.28}_{-0.23} \pm 0.08) \times 10^{-6}$ with twice the data at $60\,\text{fb}^{-1}$. Combining with the $B \to Ke^+e^-$ mode, one finds

$$\mathcal{B}(B \to K\ell^+\ell^-) = (0.58^{+0.17}_{-0.15} \pm 0.06) \times 10^{-6}, \quad (10)$$

at 5.4σ significance. These results have been confirmed [5] by the BaBar Collaboration with a dataset of $78\,\text{fb}^{-1}$, giving $\mathcal{B}(B \to K\ell^+\ell^-) = (0.78^{+0.24+0.11}_{-0.20-0.18}) \times 10^{-6}$, consistent with an earlier value of $(0.84^{+0.30+0.10}_{-0.24-0.18}) \times 10^{-6}$ at $56.4\,\text{fb}^{-1}$; the published BaBar upper limit in 2001, however, gives [4] $\mathcal{B}(B \to K\ell^+\ell^-) < 0.51 \times 10^{-6}$. The latest upper limits for $\mathcal{B}(B \to K^*\ell^+\ell^-)$ are 1.4×10^{-6} for Belle and, for BaBar, 3.0×10^{-6}, or $(1.68^{+0.68}_{-0.58} \pm 0.28) \times 10^{-6}$ at 2.8σ significance.

Given the volatility, including the muon efficiency problem of BaBar, we shall not combine the above values. However, while $\mathcal{B}(B \to K\ell^+\ell^-) \sim (0.6\text{–}0.8) \times 10^{-6}$ is not inconsistent with the SM predictions [21], it is somewhat on the high side, as we shall see. Similarly, the new Belle observation [6] of inclusive $B \to X_s\ell^+\ell^-$ decay,

$$\mathcal{B}(B \to X_s\ell^+\ell^-) = (6.1 \pm 1.4^{+1.3}_{-1.1}) \times 10^{-6}, \quad (11)$$

at 5.4σ significance, is also a bit on the high side.

We apply the same approach we have introduced for $b \to s\gamma$. Using the notations and formulas from [21], the effective Hamiltonian for $b \to s\ell^+\ell^-$ is given by

$$\mathcal{H}_{\text{eff}} = -\frac{4G_F}{\sqrt{2}} \sum_{i=1}^{i=10} [\lambda_t C_i^{\text{SM}}(\mu) + \lambda_{t'} C_i^{\text{new}}(\mu)] O_i(\mu), \quad (12)$$

where a similar decomposition as in (3) can be made. We use the Wilson coefficients C_i^{SM} calculated in naive dimensional regularization [22]. The analytic expressions for all Wilson coefficients can be found in [23]. For simplicity, we will not take into account long-distance effects from real $c\bar{c}$ intermediate states.

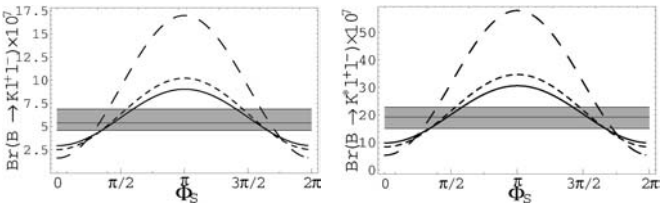

Fig. 5. Non-resonant branching ratios of $B \to K\ell^+\ell^-$ and $B \to K^*\ell^+\ell^-$, where solid, dashed and long dashed curves are for $(r_s, m_{t'}) = (0.02, 250\,\text{GeV})$, $(0.01,\ 350\,\text{GeV})$, $(0.02,\ 350\,\text{GeV})$, respectively. The horizontal band is the SM expectation at NLO using LCSR form factors, with the central line standing for the central value. The present experimental ranges are $\sim (0.5\text{–}0.8) \times 10^{-6}$ and $(0.8\text{–}1.7) \times 10^{-6}$, respectively

We work with the $\overline{\text{MS}}$ bottom mass evaluated at $\mu = 5\,\text{GeV}$. At the NLO,

$$m_b(\mu) = m_b^{\text{pole}} \left\{ 1 - \frac{4}{3}\frac{\alpha_s(\mu)}{\pi} \left(1 - \frac{3}{2}\log(m_b^{\text{pole}}/\mu) \right) \right\},$$

where $m_b^{\text{pole}} = 4.8\,\text{GeV}$ is the b quark pole mass. For the other parameters, we take $1.3\,\text{GeV}$ as the charm quark mass, $\overline{m}_t(m_t) = 168\,\text{GeV}$, $m_K = 0.497\,\text{GeV}$, $m_{K^*} = 0.896\,\text{GeV}$, $m_B = 5.28\,\text{GeV}$, $|\lambda_c| = |V_{cs}^* V_{cb}| = 0.04$ and $\sin^2\theta_W = 0.223$.

To compute the $B \to (K, K^*)\ell^+\ell^-$ rates, we need the $B \to K$ and $B \to K^*$ transition form factors, where we take the values from QCD sum rules on the light-cone (LCSR) [21].

We thus obtain the non-resonant branching ratios of $\mathcal{B}(B \to K\mu^+\mu^-) = 0.54 \times 10^{-6}$ and $\mathcal{B}(B \to K^*\mu^+\mu^-) = 1.82 \times 10^{-6}$ (compare [21]) in SM for central values of the form factors. We note that the *more recent NNLO calculations give results that are 40% smaller* [24], and could suggest the need for new physics, such as the fourth generation. For $B \to X_s l^+ l^-$, with the set of parameters chosen above, and again without including the long-distance contribution, we find that the non-resonant branching ratio within SM3 is of order 5.88×10^{-6}, where we integrate $\hat{s} = (p_{\ell^+} + p_{\ell^-})^2/m_b^2$ over the range $[4m_l^2/m_b^2, 1]$.

The strong $m_{t'}$ dependence [11] makes the electroweak penguin a particularly good probe for the presence of a fourth generation. Fourth generation contributions to $B \to (K, K^*)\ell^+\ell^-$ have been studied in [11,25]. These studies, however, took $\lambda_{t'}$ to be real, which would then be constrained by $b \to s\gamma$ to two specific $|\lambda_{t'}|$ values for a given $m_{t'}$ [13] (i.e. for $\Phi_s = 0$ and π). As we pointed out, allowing for a CP phase in $\lambda_{t'}$, for fixed $m_{t'}$ a large region in the (Φ_s, r_s) plane is actually still allowed.

In Fig. 5 we plot the non-resonant branching ratio for $B \to K\ell^+\ell^-$ and $B \to K^*\ell^+\ell^-$ versus CP phase Φ_s for several values of r_s and $m_{t'}$. The horizontal bands give the SM3 range taking into account form factor uncertainties. The pattern is similar to Δm_{B_s}: for $\cos\Phi_s > 0$ we have destructive interference, and the branching fraction is below SM; for $\cos\Phi_s < 0$ we have constructive interference and the branching ratio is largest for $\Phi_s = \pi$.

We see that the non-resonant $\mathcal{B}(B \to K\ell^+\ell^-)$ can reach approximately 2 to 3 times the SM value depend-

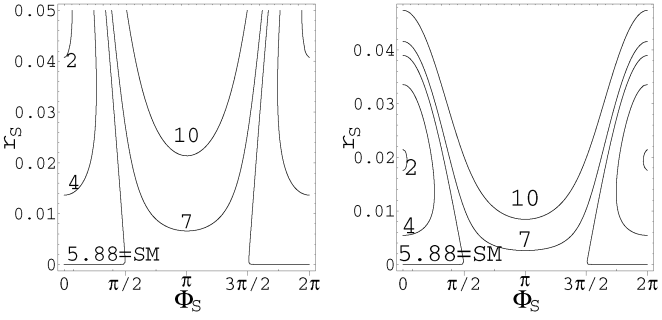

Fig. 6. Contour plot for $B \to X_s \ell^+ \ell^-$ in (Φ_s, r_s) plane for $m_{t'} = 250\ (350)\,\mathrm{GeV}$ on the left (*right*). The present experimental result is $(6.1 \pm 1.4^{+1.3}_{-1.1}) \times 10^{-6}$

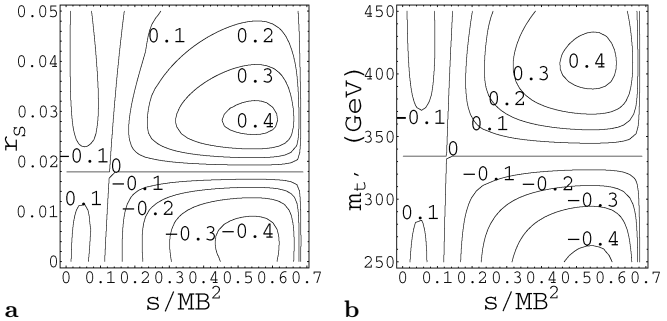

a **b**

Fig. 7a,b. Normalized forward–backward asymmetry contours for $B \to K^* \ell^+ \ell^-$, for $\Phi_s = 0$, in **a** r_s versus s/m_B^2 for $m_{t'} = 350\,\mathrm{GeV}$ and **b** $m_{t'}$ versus s/m_B^2 for $r_s = 0.02$

ing on $m_{t'}$, r_s, and Φ_s. As stated, such an enhancement may become really called for if the NNLO result [24] of $\mathcal{B}(B \to K \ell^+ \ell^-) = (0.35 \pm 0.12) \times 10^{-6}$ is borne out. In any case, a possible factor of 2–3 enhancement over SM is still within the experimental range of (10), but the case of $r_s \approx 0.02$ with $m_{t'} = 350\,\mathrm{GeV}$ may have too large a branching ratio for $\Phi_s \approx \pi$, hence $|V_{t's} V_{t'b}|$ and $m_{t'}$ should not be simultaneously too large.

Thus, the electroweak penguin modes have similar power as the Δm_{B_s} bound, which was illustrated in Fig. 2, in probing a fourth generation at present. But it may improve rapidly once the experiments converge. We note that there may be some trouble with the $\mathcal{B}(B \to K^* \ell^+ \ell^-)/\mathcal{B}(B \to K \ell^+ \ell^-)$ ratio between theory and experiment. This may be either an experimental problem (fluctuation), or a problem with form factors. For this reason, the inclusive $B \to X_s \ell^+ \ell^-$ may be more interesting, since it suffers less from hadronic uncertainties. We illustrate by a contour plot in Fig. 6 the non-resonant contribution to $\mathcal{B}(B \to X_s \ell^+ \ell^-) \times 10^6$ in the (Φ_s, r_s) plane, for $m_{t'} = 250$ and $350\,\mathrm{GeV}$. As one can see, in both cases, $\cos\Phi_s > 0$ reduces $B \to X_s l^+ l^-$ to values less than 5.88×10^{-6} and is less favored, while for $\pi/2 < \Phi_s < 3\pi/2$ the branching ratio is enhanced and grows with r_s. The behavior is similar to B_s mixing. We note that the effect of the fourth generation on $B \to X_s \ell^+ \ell^-$ has been studied recently in [14]. The constraints we obtain on r_s from $B \to X_s \ell^+ \ell^-$ are consistent with [14].

The dilepton invariant mass spectrum does not contain further information beyond the rates themselves. With proper rescaling, the shape is the same as in SM.

Let us now discuss the forward–backward asymmetry (FBA) of $B \to K^* \ell^+ \ell^-$. The usual definition is [21]

$$\frac{\mathrm{d}\mathcal{A}_{\mathrm{FB}}}{\mathrm{d}\hat{s}} = -\int_0^{\hat{u}(\hat{s})} \mathrm{d}\hat{u} \frac{\mathrm{d}^2\Gamma}{\mathrm{d}\hat{u}\mathrm{d}\hat{s}} + \int_{-\hat{u}(\hat{s})}^0 \mathrm{d}\hat{u} \frac{\mathrm{d}^2\Gamma}{\mathrm{d}\hat{u}\mathrm{d}\hat{s}}, \quad (13)$$

where $\hat{u}(\hat{s}) = \sqrt{(1 - 4\hat{m}_\ell^2/\hat{s})\lambda}$ and $\lambda = \lambda(1, \hat{m}_{K^*}^2, \hat{s}) = 1 + \hat{m}_{K^*}^4 + \hat{s}^2 - 2\hat{s} - 2\hat{m}_{K^*}^2(1 + \hat{s})$ with $\hat{m^2} = m^2/M_B^2$.

From the experimental point of view the normalized FBA ($\bar{\mathcal{A}}_{\mathrm{FB}}$) is more useful and is defined by

$$\frac{\mathrm{d}\bar{\mathcal{A}}_{\mathrm{FB}}}{\mathrm{d}\hat{s}} = \frac{\mathrm{d}\mathcal{A}_{\mathrm{FB}}}{\mathrm{d}\hat{s}} \Big/ \frac{\mathrm{d}\Gamma}{\mathrm{d}\hat{s}}. \quad (14)$$

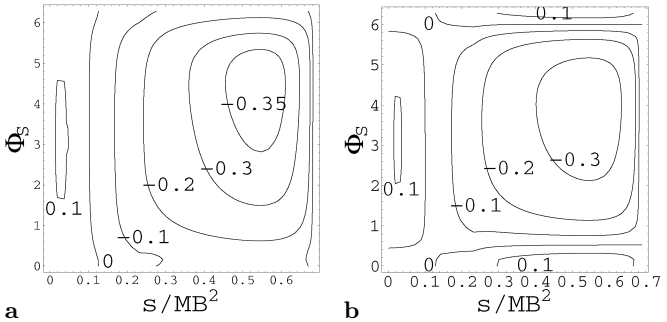

a **b**

Fig. 8a,b. Normalized $B \to K^* \ell^+ \ell^-$ forward–backward asymmetry contours for Φ_s versus s/m_B^2, for **a** $m_{t'} = 250\,\mathrm{GeV}$, $r_s = 0.04$, and **b** $m_{t'} = 350\,\mathrm{GeV}$, $r_s = 0.02$

Note that the FBA for $B \to K \ell^+ \ell^-$ vanishes.

In the SM, the FBA for $B \to K^* \ell^+ \ell^-$ is positive for $\hat{s} < 0.1$ with values going up to ≈ 0.1, vanishes at $\hat{s}_0 = 0.1$ and turns negative for $0.7 > \hat{s} > 0.1$ with FBA values going down to ≈ -0.4. This reflects the interference between the $b \to s\gamma^*$ versus $b \to sZ^*$ mediated processes. The presence of a fourth generation affects the latter more strongly and hence can change the pattern. We are interested in the parameter space where the shape of FBA changes completely from that of SM. In Fig. 7, we give contour plots for normalized FBA, for $\Phi_s = 0$, in the $(\hat{s}, r_s)$ plane for $m_{t'} = 350\,\mathrm{GeV}$ (left) and in the $(\hat{s}, m_{t'})$ plane for $r_s = 0.02$ (right). We see that FBA can vanish not only for $\hat{s} = 0.1$ but also in the full range of $0.7 > \hat{s} > 0.1$. In the left plot this happens for $r_s^0 \approx 0.018$ and $m_{t'} = 350\,\mathrm{GeV}$ while in the right plot this seems to happen for $m_{t'}^0 \approx 335\,\mathrm{GeV}$ and $r_s = 0.02$. From the left contour, note that for $r_s < r_s^0$, the FBA is negative for $\hat{s} > 0.1$ exactly as in the SM, but for $r_s > r_s^0$, the FBA remains positive even for $\hat{s} > 0.1$. The same observation can be made for $\hat{s} > 0.1$ in the right contour: the FBA is negative for $m_{t'} < m_{t'}^0$ but positive for $m_{t'} > m_{t'}^0$, and FBA can reach $+0.4$ or more.

In Fig. 8, we illustrate the effect of the CP phase Φ_s for normalized FBA in the $(\hat{s}, \Phi_s)$ plane for $m_{t'} = 250\,\mathrm{GeV}$, $r_s = 0.04$ (left), and for $m_{t'} = 350\,\mathrm{GeV}$, $r_s = 0.02$ (right). From the left plot, one can see that FBA has a constant sign (negative) for large $\hat{s} > 0.1$ and can become larger than -0.3 for a large CP phase and large $\hat{s}$. In the right

plot the FBA can flip sign for $\Phi_s \approx 0.5$ and for values of $\hat{s} > 0.1$.

5 CP-violation in charmless B decays

Although it is too early to draw conclusions [26], both Belle and BaBar presented [7] some hints for mixing-dependent CP violation in the charmless $B^0 \to \phi K_S$ decay mode, with the two experiments agreeing in sign. It is intriguing that *the sign is opposite to that of* $B^0 \to J/\psi K_S$*!* We do not advocate that new physics is already called for, but illustrate the impact of a fourth generation.

It is known that the CP asymmetry in both $B^0 \to \phi K_S$ and $J/\psi K_S$ should measure the same quantity $\sin 2\phi_1$ in SM, where the uncertainty is estimated to be less than $\mathcal{O}(\lambda^2)$ [28].

The effective Hamiltonian for the $\Delta B = 1$ transition can be written as [27]

$$\mathcal{H}_{\rm eff} = \frac{G_F}{\sqrt{2}} \left\{ \lambda_u (C_1 O_1^u + C_2 O_2^u) + \lambda_c (C_1 O_1^c + C_2 O_2^c) - \sum_{i=3}^{i=10} [\lambda_t C_i^{\rm SM}(\mu) + \lambda_{t'} C_i^{\rm new}(\mu)] O_i(\mu) \right\}. \quad (15)$$

For the SM part, we have used the next-to-leading order formulas given in [27] for the Wilson coefficients, while for the fourth generation effect in $C_i^{\rm new}$, we have used the leading order analytic formulas given in [29].

Following the notation of [27], in the factorization approach, the amplitude of both $B^- \to K^- \phi$ and $\bar{B}^0 \to \bar{K}^0 \phi$ is proportional to $V_{tb} V_{ts}^* (a_3 + a_4 + a_5 - 1/2(a_7 + a_9 + a_{10}))$. The exact form of the factorizable hadronic matrix element is irrelevant for us since we are interested only in CP asymmetry observables in SM4, and the ratio of the branching ratios in SM3 and SM4. The coefficients a_i are defined by $a_i = C_i^{\rm eff} + 1/N_C C_{i\pm1}^{\rm eff}$ for odd, even i.

The CP asymmetry $\sin(2\Phi_{\phi K_S})$ is defined by

$$\sin(2\Phi_{\phi K_S}) = -\frac{2\,{\rm Im}\,\Lambda}{1 + |\Lambda|^2}, \quad (16)$$

where $\Lambda = {\rm e}^{-2{\rm i}\phi_1} (\overline{\mathcal{A}}/\mathcal{A})$ with $\overline{\mathcal{A}}$ being the CP-conjugate amplitude of $\mathcal{A}$. We define also the following ratio:

$$R_{\phi K_S} = \frac{\mathcal{A}_{\rm SM4}(B^0 \to \phi K_S)}{\mathcal{A}_{\rm SM3}(B^0 \to \phi K_S)}. \quad (17)$$

In our analysis we use the following set of parameters: $\mu = 2.5\,{\rm GeV}$, $m_t = 168\,{\rm GeV}$, $m_b = 4.88\,{\rm GeV}$, $k^2 = m_b^2/2$, $\alpha = 1/128$ and $s_W^2 = 0.223$ and $\alpha_s(M_W) = 0.118$.

In SM3 (i.e. without a fourth generation) we find that $\overline{\mathcal{A}}/\mathcal{A} = 0.979$, which is close to 1, and which means that $\sin 2\Phi_{\phi K_S} \cong \sin 2\phi_1 = \sin 2\Phi_{J/\psi K_S}$. In our numerical evaluation we take ϕ_1 close to 24° which reproduces the world average of $\sin 2\phi_1 = 0.734$ coming from $B^0 \to J/\psi K_S$.

IN SM4, the ratio $\overline{\mathcal{A}}/\mathcal{A}$ has an additional CP phase, which we denote 2θ, that arises from our CP phase Φ_s.

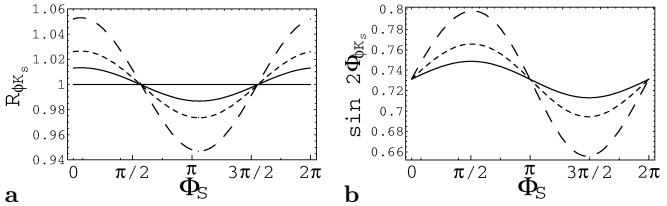

Fig. 9. **a** Ratio $R_{\phi K_S}$ and **b** $\sin(2\Phi_{\phi K_S})$ as a function of the CP phase Φ_s, where solid, dashed and long dashed curves are for $r_s = 0.01$, 0.02 and 0.04, respectively, with $m_{t'} = 400\,{\rm GeV}$

So if we use the definition of Λ defined above,

$$\Lambda = {\rm e}^{-2{\rm i}\phi_1} \frac{\overline{\mathcal{A}}}{\mathcal{A}} = {\rm e}^{-2{\rm i}(\phi_1 + \theta)} \left| \frac{\overline{\mathcal{A}}}{\mathcal{A}} \right|, \quad (18)$$

where we have used $\overline{\mathcal{A}}/\mathcal{A} = {\rm e}^{-{\rm i}2\theta} |\overline{\mathcal{A}}/\mathcal{A}|$.

We have studied numerically the effect of the CP phase Φ_s, r_s and $m_{t'}$ on both $\sin(2\Phi_{\phi K_S})$ and $R_{\phi K_S}$ and found that for $r_s < 0.05$ and $m_{t'} \le 450\,{\rm GeV}$ the effect is rather small. In Fig. 9 we illustrate the effect of Φ_s on $R_{\phi K_S}$ (left) and $\sin(2\Phi_{\phi K_S})$ (right) for $m_{t'} = 400\,{\rm GeV}$ and several values for r_s. For $r_s = 0.02$, $B^0 \to \phi K_S$ in SM4 can be enhanced (reduced) only by about 2% for $\cos\Phi_s > 0$ (< 0). For large $r_s = 0.04$, the effect can only reach about 5%. As one can see in the right plot, the effect of the CP phase Φ_s on $\sin(2\Phi_{\phi K_S})$ is also not impressive. Both in SM3 and SM4, we find numerically that $a_4 \gg a_9/2$ for all Φ_s, while $a_3 \gg a_7/2$ and $a_5 \gg a_{10}/2$ in the region where $\cos\Phi_s$ is not close to 1 ($\Phi_s \neq 0$ and 2π). It can be seen that $\sin(2\Phi_{\phi K_S})$ is enhanced for $0 < \Phi_s < \pi$ and reduced for $\pi < \Phi_s < 2\pi$. For $r_s = 0.02$ (0.04) the enhancement (suppression) is about +15% (−30%). The suppression of $\sin(2\Phi_{\phi K_S})$ is insufficient to drive it negative, even for rather sizable r_s. For sign change, one would need $\Phi_s \simeq 3\pi/2$ with an unacceptably large r_s. For example, for $m_{t'} = 400\,{\rm GeV}$ and $\Phi_s = 3\pi/2$, $\sin 2\Phi_{\phi K_S}$ turns negative for $r_s > 0.11$, which is much larger than V_{cb}.

6 Discussion and conclusion

A particularly interesting aspect of the existence of a fourth sequential generation is the presence of new CP-violating phases. Restricting ourselves to $b \to s$ transitions, besides the strength of $|V_{t's} V_{t'b}| \equiv r_s$, one has a unique new CP phase, $\arg V_{t's} V_{t'b} \equiv \Phi_s$. Existing work in the literature has not emphasized the $\Phi_s \neq 0$, π situation, hence has overconstrained the possible impact of the fourth generation. In the present work, we have tried to cover as much ground as possible, and we find a rather enriched phenomenology for the $b \to s$ transitions, for both CP-violating or CP-independent observables.

The $b \to s\gamma$ process is not very sensitive to the presence of a fourth generation, since the structure is rather similar to SM, and it is not possible to generate a large CP asymmetry because of the chiral structure. It is therefore especially accommodating for $\Phi_s = \pi/2$, $3\pi/2$, when the fourth generation contribution adds only in quadrature in

rate. These are the most interesting situations, since CP-violating effects elsewhere are the *largest*.

For example, B_s mixing and the CP phase $\sin 2\Phi_{B_s}$ are very interesting probes of fourth generation effects. While some part of the parameter space allowed by $b \to s\gamma$ ($\cos\Phi_s \gtrsim 0$) is ruled out, Δm_{B_s} can be much larger than SM3 expectations. Any value for $\sin 2\Phi_{B_s}$ between -1 and $+1$ is in principle possible. What may be interesting is that, even for r_s rather small, hence Δm_{B_s} just above the present bound, $\sin 2\Phi_{B_s}$ could still be sizable. Thus, Tevatron Run II data are eagerly awaited.

The electroweak penguin modes $B \to K^{(*)}\ell^+\ell^-$ and $X_s\ell^+\ell^-$ have recently been observed, and the rates tend to be a little on the high side, especially when compared to more recent NNLO results. Again, the best case seems to be for $\Phi_s \sim \pi/2,\ 3\pi/2$, when fourth generation effects add mildly in quadrature. Although the dilepton spectrum, and roughly speaking the direct CP asymmetries as well (analogous to $b \to s\gamma$), are not much affected, the forward–backward asymmetry, $\mathcal{A}_{\rm FB}$, can be drastically affected. This is because the γ^* effect is far less sensitive to fourth generation effects than the Z^* effect, so the $s = m^2_{\ell^+\ell^-}/m^2_B$ dependence of $\mathcal{A}_{\rm FB}$ is a sensitive probe of the interference between the two terms. Thus, while we need the Belle and BaBar measured rates to converge better, in the long run the forward–backward asymmetry may provide a very interesting probe of the fourth generation.

Finally, we studied the mixing-dependent CP-violation in the $B \to \phi K_{\rm S}$ charmless decay, since some hint for physics beyond SM appeared here recently. We found the effect of a fourth generation to be insignificant here. This is because the strong penguin, even more so than $b \to s\gamma$, depends very mildly on the fourth generation, while the "harder" C_9 term, analogous to the electroweak penguin contribution to $B \to K^{(*)}\ell\ell$, is subdominant. Thus, even with its new source of CP-violation, it is unlikely for the fourth generation to change the sign of $\sin 2\Phi_{\phi K_{\rm S}}$ with respect to $\sin 2\Phi_{J/\psi K_{\rm S}}$ in the B_d system.

The impact of the fourth generation is most prominent in B_s mixing and electroweak penguin $b \to s$ transitions, but mild in electromagnetic and strong penguins. We have found that the fourth generation, even with $|V_{t's}V_{t'b}|$ not far below $|V_{cs}V_{cb}| \simeq 0.04$, could be lurking with a purely imaginary KM phase.

Acknowledgements. A. Arhrib is supported by the Alexander von Humboldt Foundation. The work of WSH is supported in part by grant NSC-91-2112-M-002-027, the MOE CosPA Project, and the BCP Topical Program of NCTS.

References

1. P.H. Frampton, P.Q. Hung, M. Sher, Phys. Rept. **330**, 263 (2000); J.I. Silva-Marcos, hep-ph/0204217
2. K. Abe et al. [BELLE Collaboration], Phys. Rev. Lett. **88**, 021801 (2002)
3. K. Abe et al. [BELLE Collaboration], BELLE-CONF-0241, contributed to 31st International Conference on High Energy Physics (ICHEP 2002), Amsterdam, The Netherlands, 24–31 July 2002 (see talk by S. Nishida)
4. B. Aubert et al. [BABAR Collaboration], Phys. Rev. Lett. **88**, 241801 (2002)
5. B. Aubert et al. [BABAR Collaboration], hep-ex/0207082, contributed to ICHEP 2002
6. J. Kaneko et al. [Belle Collaboration], hep-ex/0208029, submitted to Phys. Rev. Lett.
7. Plenary talk by M. Yamauchi (Belle Collaboration) at ICHEP 2002; B. Aubert et al. [BABAR Collaboration], hep-ex/0207070, contributed to ICHEP 2002 (see talk by J. Richman)
8. M.S. Alam et al. [CLEO Collaboration], Phys. Rev. Lett. **74**, 2885 (1995)
9. M. Ciuchini, G. Degrassi, P. Gambino, G.F. Giudice, Nucl. Phys. B **527**, 21 (1998); F.M. Borzumati, C. Greub, Phys. Rev. D **59**, 057501 (1999)
10. W.S. Hou, A. Soni, H. Steger, Phys. Lett. B **192**, 441 (1987)
11. W.S. Hou, R.S. Willey, A. Soni, Phys. Rev. Lett. **58**, 1608 (1987) [Erratum-ibid. **60**, 2337 (1987)]
12. T. Hattori, T. Hasuike, S. Wakaizumi, Phys. Rev. D **60**, 113008 (1999); T.M. Aliev, D.A. Demir, N.K. Pak, Phys. Lett. B **389**, 83 (1996); Y. Dincer, Phys. Lett. B **505**, 89 (2001) and references therin
13. C.S. Huang, W.J. Huo, Y.L. Wu, Mod. Phys. Lett. A **14**, 2453 (1999); C.S. Huang, W.J. Huo, Y.L. Wu, Phys. Rev. D **64**, 016009 (2001)
14. T. Yanir, JHEP **0206**, 044 (2002)
15. K. Hagiwara et al. [Particle Data Group Collaboration], Phys. Rev. D **66**, 010001 (2002)
16. A.J. Buras et al., Nucl. Phys. B **424**, 374 (1994); C.K. Chua, X.G. He, W.S. Hou, Phys. Rev. D **60**, 014003 (1999)
17. T. Affolder et al. [CDF Collaboration], Phys. Rev. Lett. **84**, 835 (2000)
18. A. Arhrib, W.S. Hou, Phys. Rev. D **64**, 073016 (2001)
19. P.H. Frampton, P.Q. Hung, M. Sher, Phys. Rept. **330**, 263 (2000); H.J. He, N. Polonsky, S. f. Su, Phys. Rev. D **64**, 053004 (2001); V.A. Novikov, L.B. Okun, A.N. Rozanov, M.I. Vysotsky, Phys. Lett. B **529**, 111 (2002)
20. T. Inami, C.S. Lim, Prog. Theor. Phys. **65**, 297 (1981) [Erratum-ibid. **65**, 1772 (1981)]
21. A. Ali, P. Ball, L.T. Handoko, G. Hiller, Phys. Rev. D **61**, 074024 (2000)
22. A.J. Buras, M. Misiak, M. Munz, S. Pokorski, Nucl. Phys. B **424**, 374 (1994)
23. G. Buchalla, A.J. Buras, M.E. Lautenbacher, Rev. Mod. Phys. **68**, 1125 (1996); A.J. Buras, M. Munz, Phys. Rev. D **52**, 186 (1995)
24. A. Ali, E. Lunghi, C. Greub, G. Hiller, Phys. Rev. D **66**, 034002 (2002)
25. T.M. Aliev, A. Ozpineci, M. Savci, Nucl. Phys. B **585**, 275 (2000)
26. Y. Nir, hep-ph/0208080, plenary talk presented at ICHEP 2002
27. A. Ali, G. Kramer, C.D. Lu, Phys. Rev. D **58**, 094009 (1998)
28. Y. Grossman, M.P. Worah, Phys. Lett. B **395**, 241 (1997); Y. Grossman, G. Isidori, M.P. Worah, Phys. Rev. D **58**, 057504 (1998)
29. M. Ciuchini, E. Franco, G. Martinelli, L. Reina, Nucl. Phys. B **415**, 403 (1994); A.J. Buras, M. Jamin, M.E. Lautenbacher, P.H. Weisz, Nucl. Phys. B **370**, 69 (1992) [Addendum-ibid. B **375**, 501 (1992)]